Photoluminescent Properties and Molecular Structure of $[\{Au(PPh_3)\}_2(\mu\text{-bbzim})]$ and $[\{Au(PPh_3)\}_4(\mu\text{-bbzim})][ClO_4]_2$ (bbzim = 2,2'-Bibenzimidazolate)†

Biing-Chiau Tzeng,[a] Dan Li,[b] Shie-Ming Peng*[,a] and Chi-Ming Che*[,a,b]

[a] *Department of Chemistry, National Taiwan University, Taipei, Taiwan*

[b] *Department of Chemistry, The University of Hong Kong, Pokfulam Road, Hong Kong*

The tetranuclear $[\{Au(PPh_3)\}_4(\mu\text{-bbzim})][ClO_4]_2$ and dinuclear $[\{Au(PPh_3)\}_2(\mu\text{-bbzim})]$ complexes with 2,2'-bibenzimidazolate (bbzim) as bridging ligand have been characterized by X-ray crystallography. The intramolecular Au–Au separations in $[\{Au(PPh_3)\}_4(\mu\text{-bbzim})][ClO_4]_2$ are 3.157(1)–3.222(1) Å. Upon excitation at 330 nm, both complexes display intense intraligand fluorescence and phosphorescence in fluid solution at room temperature.

The large number of readily available polynuclear d^{10} metal complexes has greatly encouraged photophysical and spectroscopic studies of them. Recently, there have been extensive works on the luminescent properties of gold(I) complexes with bridging phosphine ligands,[1–3] the emissive excited states of which have been suggested to arise from the metal-centred 5d ⟶ (6s, 6p) state[2,3] or gold ⟶ phosphine charge-transfer transitions.[1]

Only a few gold(I) amido complexes have been reported. In the present paper we describe the molecular structure and photophysical properties of di- and tetra-nuclear amidogold(I) complexes, $[\{Au(PPh_3)\}_2(\mu\text{-bbzim})]$ **1** and $[\{Au(PPh_3)\}_4(\mu\text{-bbzim})][ClO_4]_2$ **2**, in which the anion $bbzim^{2-}$ acts as a bridging ligand (2,2'-bibenzimidazolate). Their emissive excited states have been assigned to intraligand fluorescence and phosphorescence with gold(I) perturbation.

Experimental

Materials.—The complex $[Au(PPh_3)Cl]$ was purchased from Strem Chemicals and all solvents (analytical grade) for synthesis were used without further purification. Solvents for photophysical studies were purified by literature methods. The compounds H_2bbzim,[4] $[\{Au(PPh_3)\}_2(\mu\text{-bbzim})]$[5] and $[\{Au(PPh_3)\}_4(\mu\text{-bbzim})][ClO_4]_2$[5] were synthesised by literature methods.

$[\{Au(PPh_3)\}_2(\mu\text{-bbzim})]$. A solution of $[Au(PPh_3)Cl]$ in CH_2Cl_2–MeOH (1:2, 30 cm^3) was stirred with $Na_2(bbzim)$ [obtained from H_2bbzim (0.1 mmol) and NaOMe (0.2 mmol) in CH_2Cl_2–MeOH (1:1, 30 cm^3)] for 24 h. Upon standing for several days, pale yellow crystals of $[\{Au(PPh_3)\}_2(\mu\text{-bbzim})]$ suitable for X-ray diffraction analysis were obtained.

$[\{Au(PPh_3)\}_4(\mu\text{-bbzim})][ClO_4]_2$. To a solution of $[Au(PPh_3)]ClO_4$ (0.2 mmol) {obtained by treating $[Au(PPh_3)Cl]$ with $AgClO_4$} in CH_2Cl_2–MeOH (1:2, 30 cm^3) was added $[\{Au(PPh_3)\}_2(\mu\text{-bbzim})]$ (0.1 mmol). After stirring for 12 h the solution became colourless. Colourless crystals were obtained by diffusing diethyl ether into the solution.

Physical Measurements and Instrumentation.—The UV/VIS spectra were recorded on a Milton Roy Spectronic 3000 diode-array spectrophotometer and steady-state emission spectra on a SPEX Fluorolog-2 spectrofluorometer. Emission lifetime measurements were performed with a Quanta Ray DCR-3 Nd-YAG laser (pulse output 355 nm, 8 ns). The decay signal was recorded by a R928 PMT (Hamamatsu) digitized with a Tektronix 2430 digital oscilloscope interfaced to an IBM PC/AT computer, equipped with single-exponential fitting. Solutions for photochemical experiments were degassed by at least four freeze–pump–thaw cycles. The self-quenching rate constants k_q were obtained from Stern–Volmer plots $1/t = (1/t_0) + k_q c$ where c is the concentration of ligand or metal complex.

Crystal-structure Determinations.—$[\{Au(PPh_3)\}_2(\mu\text{-bbzim})]\cdot H_2O$. X-Ray diffraction data were collected on an Enraf–Nonius CAD-4 four-circle diffractometer (graphite-monochromatized Mo-Kα radiation) using the θ–2θ scan mode. The cell dimensions were obtained from a least-squares fit of 25 reflections in the range $18 < 2\theta < 26°$. The data were corrected for ψ-scan absorption. Crystallographic data are summarized in Table 1.

$[\{Au(PPh_3)\}_4(\mu\text{-bbzim})][ClO_4]_2$. X-Ray diffraction data were collected on a Rigaku diffractometer (graphite-monochromatized Cu-Kα radiation) using the θ–2θ scan mode. The cell dimensions were obtained from a least-squares fit of 25 reflections in the range $100 < 2\theta < 120°$. The data were corrected for ψ-scan absorption. Crystallographic data are summarized in Table 1.

All the data reduction and structural refinement was performed using the NRCC-SDP-VAX packages.[6] The structures were solved by the Patterson method and refined by least-squares cycles. All non-hydrogen atoms were refined with anisotropic thermal parameters. Hydrogen atoms were included at idealized positions with a fixed isotropic thermal parameter $U_H = U_C + 0.01$ Å^2.

The final agreement factors are given in Table 1. Atomic coordinates of non-hydrogen atoms are listed in Tables 2 and 3 and selected bond distances and angles in Tables 4 and 5.

Additional material available from the Cambridge Crystallographic Data Centre comprises H-atom coordinates, thermal parameters and remaining bond lengths and angles.

Results and Discussion

Crystallographic Results.—The molecular units found in the crystals of $[\{Au(PPh_3)\}_2(\mu\text{-bbzim})]$ and $[\{Au(PPh_3)\}_4(\mu\text{-bbzim})]^{2+}$ are shown in Figs. 1 and 2. In $[\{Au(PPh_3)\}_2(\mu\text{-bbzim})]$ the $bbzim^{2-}$ ligand bridges two gold atoms through

† *Supplementary data available:* see Instructions for Authors, *J. Chem. Soc., Dalton Trans.*, 1993, Issue 1, pp. xxiii–xxviii.

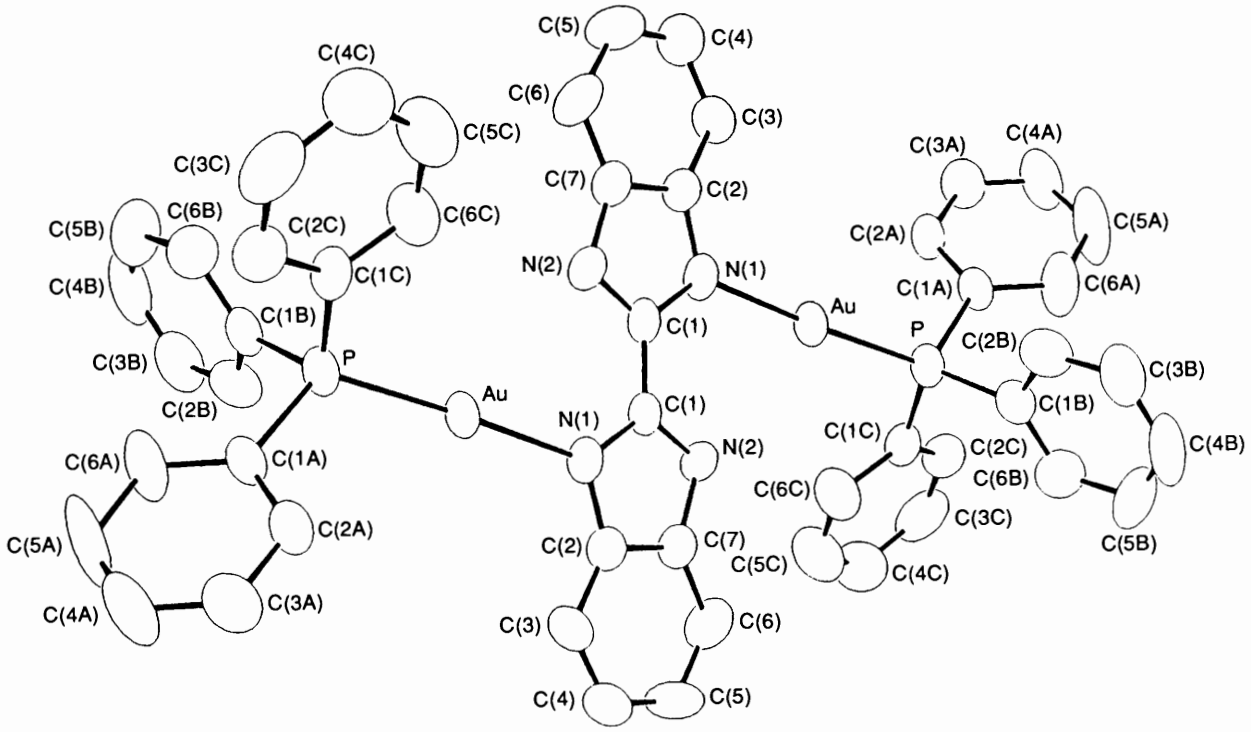

Fig. 1 A perspective view of $[\{Au(PPh_3)\}_2(\mu\text{-bbzim})]$ showing the atom numbering

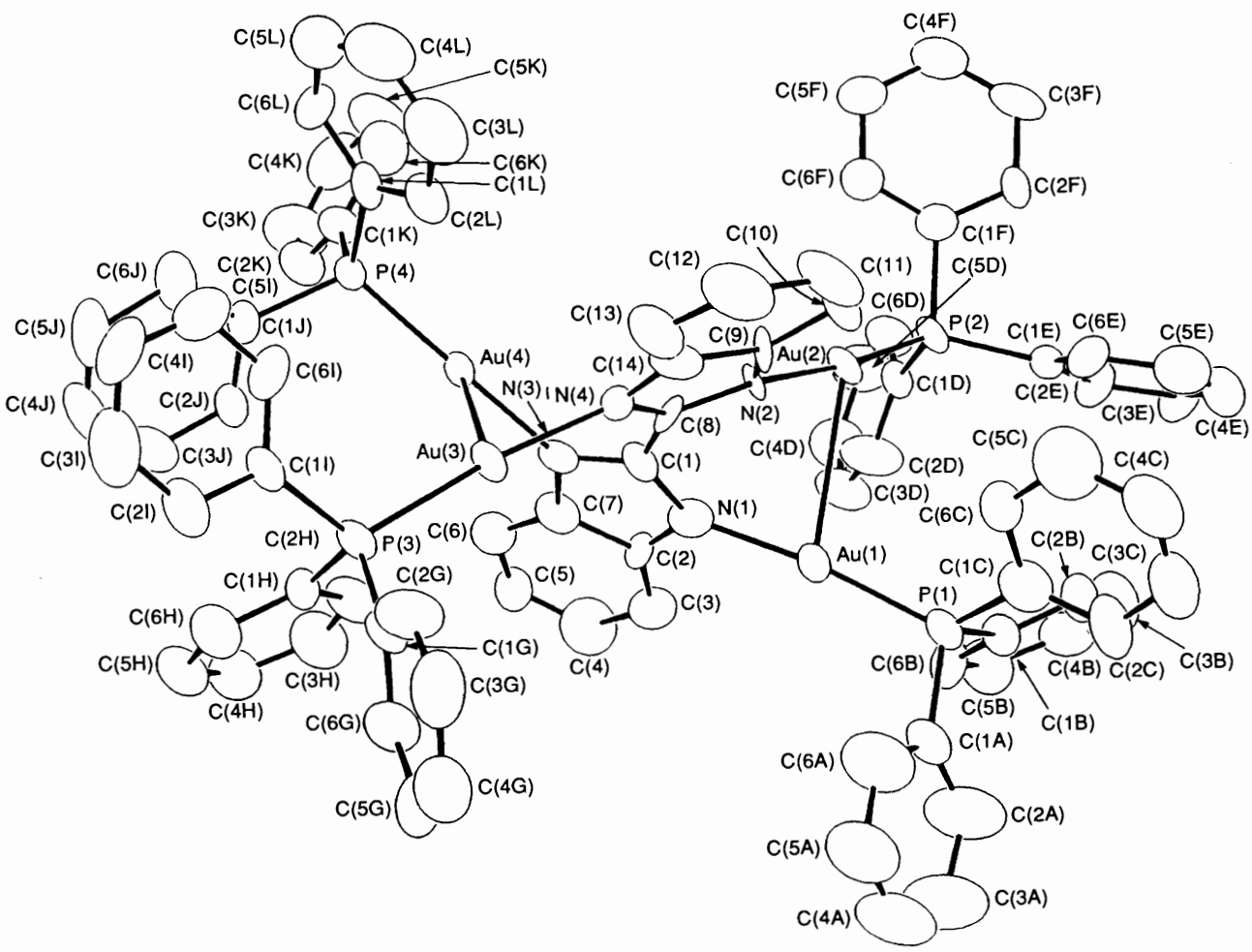

Fig. 2 A perspective view of $[\{Au(PPh_3)\}_4(\mu\text{-bbzim})]^{2+}$ showing the atom numbering

Table 1 Crystallographic data for $[\{Au(PPh_3)\}_2(\mu\text{-bbzim})]\cdot H_2O$ and $[\{Au(PPh_3)\}_4(\mu\text{-bbzim})][ClO_4]_2\cdot CH_2Cl_2\cdot OEt_2$

	$[\{Au(PPh_3)\}_2(\mu\text{-bbzim})]$	$[\{Au(PPh_3)\}_4(\mu\text{-bbzim})][ClO_4]_2$
Formula	$C_{50}H_{40}Au_2N_4OP_2$	$C_{92}H_{82}Au_4Cl_6N_4O_9P_4$
M	1168.77	2512.13
Space group	$P\bar{1}$	$P2_1/n$
a/Å	9.188(4)	18.678(5)
b/Å	9.493(5)	12.473(3)
c/Å	14.044(5)	39.642(6)
α/°	71.79(4)	
β/°	78.76(3)	92.56(3)
γ/°	82.81(4)	
U/Å^3	1138.6(9)	9226(4)
Z	1	4
D_c/mg m^{-3}	1.705	1.809
μ/cm^{-1}	6.52 (Mo-Kα)	13.48 (Cu-Kα)
λ/Å	0.7107	1.5406
$2\theta_{max}$/°	45	120.0
Crystal dimension (mm)	0.05 × 0.17 × 0.55	0.15 × 0.20 × 0.40
$F(000)$	564	4343
No. of unique reflections	2969	12 534
No. of reflections with $I > 2\sigma(I)$	2589	8541
Weighting scheme	$w^{-1} = \sigma^2(F) + 0.0001F^2$	$w^{-1} = \sigma(F)$
R^a	0.034	0.070
R'^b	0.040	0.079
Goodness of fit^c	3.58	2.14
Residual extrema in final difference map/e Å^{-3}	−1.14, 132	−3.23, 2.35

^{a} $\Sigma||F_o| - |F_c||/\Sigma|F_o|$. ^{b} $[\Sigma w(|F_o| - |F_c|)^2/\Sigma w(|F_o|)^2]^{\frac{1}{2}}$. ^{c} $[\Sigma w(|F_o| - |F_c|)^2/(N_r - N_p)]^{\frac{1}{2}}$ (N_r = no. of reflections, N_p = no. of variables).

Table 2 Non-hydrogen atom coordinates for $[\{Au(PPh_3)\}_2(\mu\text{-bbzim})]$ with estimated standard deviations (e.s.d.s) in parentheses

Atom	x	y	z
Au	0.251 22(6)	0.259 95(5)	0.087 24(5)
P	0.315 1(3)	0.054 3(3)	0.204 9(3)
N(1)	0.201 8(10)	0.446 4(9)	−0.026 8(8)
N(2)	0.058 4(9)	0.608 0(9)	−0.132 4(8)
C(1)	0.062 5(11)	0.514 6(11)	−0.041 0(9)
C(2)	0.295 2(13)	0.502 6(12)	−0.119 1(10)
C(3)	0.446 8(13)	0.480 3(13)	−0.148 7(11)
C(4)	0.507 4(14)	0.554 0(14)	−0.245 6(12)
C(5)	0.420 9(15)	0.647 4(16)	−0.310 9(12)
C(6)	0.269 8(15)	0.673 2(14)	−0.282 0(11)
C(7)	0.203 5(13)	0.602 2(12)	−0.184 7(10)
C(1A)	0.513 1(11)	−0.002 7(11)	0.191 9(9)
C(2A)	0.613 3(13)	0.102 3(12)	0.159 3(11)
C(3A)	0.764 3(13)	0.061 3(14)	0.150 3(12)
C(4A)	0.814 7(13)	−0.079 4(14)	0.173 0(13)
C(5A)	0.716 2(15)	−0.185 7(14)	0.201 6(15)
C(6A)	0.563 5(13)	−0.148 7(13)	0.214 6(13)
C(1B)	0.227 9(12)	−0.110 4(12)	0.208 6(10)
C(2B)	0.235 5(13)	−0.145 3(13)	0.120 1(11)
C(3B)	0.181 6(14)	−0.272 8(13)	0.119 6(12)
C(4B)	0.118 7(14)	−0.368 2(13)	0.208 4(13)
C(5B)	0.109 3(15)	−0.335 4(13)	0.295 6(13)
C(6B)	0.163 6(14)	−0.206 9(13)	0.298 2(11)
C(1C)	0.261 4(12)	0.077 1(11)	0.327 8(9)
C(2C)	0.336 6(14)	0.004 2(13)	0.405 7(10)
C(3C)	0.291 5(15)	0.027 1(15)	0.502 7(11)
C(4C)	0.168 3(17)	0.123 1(16)	0.523 1(12)
C(5C)	0.097 7(16)	0.197 0(16)	0.440 5(13)
C(6C)	0.141 7(14)	0.175 4(14)	0.343 9(11)
O	0.362(3)	0.490(3)	0.508 2(18)

the two imidazole nitrogen atoms at opposite sides. The co-ordination at each Au atom is essentially linear [P–Au–N 176.9(3)°] and is similar to that [177(1), 173(1)°] in $[\{Au(PPh_3)\}_2(\mu\text{-bbzim})Rh(cod)]ClO_4\cdot CHCl_3$ **3** (cod = cycloocta-1,5-diene).[7]

In $[\{Au(PPh_3)\}_4(\mu\text{-bbzim})]^{2+}$ the $bbzim^{2-}$ dianion acts as a tetradentate ligand, which co-ordinates to four gold(I) atoms in an unsymmetrical manner. The two Au atoms at each side of the bbzim^{2-} ligand approach each other quite closely with Au(1)–Au(2) and Au(3)–Au(4) separations being 3.157(1) and 3.222(1) Å respectively. These values are comparable to the intramolecular Au–Au separation in complex **3**. The N–Au–P angles which lie in the range 171.2(4)–174.7(5)° are slightly less than those found in $[\{Au(PPh_3)\}_2(\mu\text{-bbzim})]$ and in **3**. Both benzimidazolate rings in the bbzim^{2-} ligand are strictly planar and are significantly twisted with respect to each other with a dihedral angle of 41.6(8)°. The corresponding dihedral angle in **3** is 17.6°.

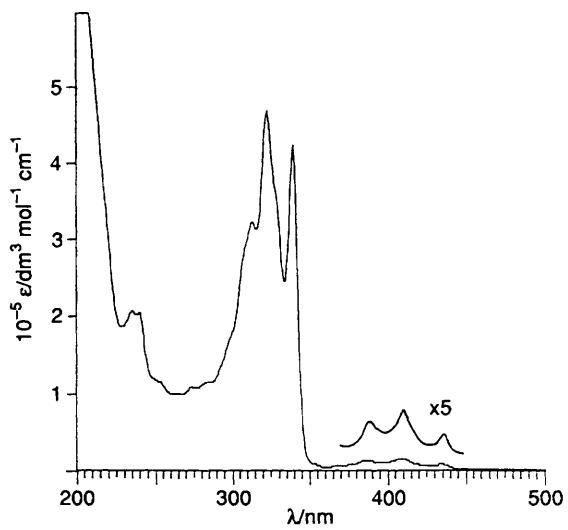

Fig. 3 The UV/VIS absorption spectrum of H_2bbzim in MeCN at room temperature

The Au–N and Au–P distances are very similar in $[\{Au(PPh_3)\}_2(\mu\text{-bbzim})]$ [Au–N 2.053(9), Au–P 2.228(3) Å] and $[\{Au(PPh_3)\}_4(\mu\text{-bbzim})]^{2+}$ [Au–N 2.028(7)–2.061(16), Au–P 2.233(5)–2.239(5) Å] as well as in **3** [Au–N 1.96(3) and 1.98(3), Au–P 2.23(1) and 2.22(1) Å].

Photophysical Properties of the Free Ligand.—Fig. 3 shows the electronic absorption spectrum of H_2bbzim measured in acetonitrile, which features an intense vibronic structured absorption band at 280–350 nm. This band is assigned to the

Table 3 Non-hydrogen atom coordinates for $[\{Au(PPh_3)\}_4(\mu\text{-bbzim})][ClO_4]_2$ with e.s.d.s in parentheses

Atom	x	y	z	Atom	x	y	z
Au(1)	0.251 15(4)	0.230 31(8)	0.127 576(21)	C(5F)	0.226 4(13)	0.641 3(20)	−0.022 7(6)
Au(2)	0.265 17(4)	0.354 66(8)	0.058 833(20)	C(6F)	0.216 5(12)	0.573 2(19)	0.003 7(6)
Au(3)	0.548 04(4)	0.349 42(8)	0.143 063(21)	C(1G)	0.639 5(10)	0.198 7(16)	0.196 7(5)
Au(4)	0.478 82(4)	0.586 09(8)	0.140 932(20)	C(2G)	0.674 0(14)	0.131 9(21)	0.176 4(7)
P(1)	0.184 4(3)	0.083 7(5)	0.118 04(13)	C(3G)	0.680 6(14)	0.026 7(24)	0.183 6(8)
P(2)	0.157 0(3)	0.402 1(5)	0.037 65(12)	C(4G)	0.652 5(14)	−0.018 4(21)	0.212 1(7)
P(3)	0.629 1(3)	0.335 9(5)	0.186 19(13)	C(5G)	0.617 1(14)	0.046 4(23)	0.233 0(7)
P(4)	0.561 3(3)	0.711 8(5)	0.132 51(12)	C(6G)	0.609 9(13)	0.154 7(19)	0.225 5(6)
N(1)	0.307 6(8)	0.362 0(14)	0.142 7(4)	C(1H)	0.605 2(10)	0.406 0(16)	0.223 0(5)
N(2)	0.369 0(8)	0.323 1(14)	0.075 1(4)	C(2H)	0.533 5(12)	0.436 6(21)	0.227 5(5)
N(3)	0.397 1(8)	0.481 0(14)	0.150 6(4)	C(3H)	0.511 0(14)	0.483 3(24)	0.256 4(7)
N(4)	0.474 8(8)	0.336 7(12)	0.102 9(4)	C(4H)	0.559 5(13)	0.499 4(20)	0.282 7(6)
C(1)	0.369 3(10)	0.399 6(16)	0.131 3(5)	C(5H)	0.629 2(13)	0.466 8(20)	0.280 1(5)
C(2)	0.293 8(9)	0.420 2(16)	0.171 0(5)	C(6H)	0.650 6(12)	0.418 4(20)	0.251 3(6)
C(3)	0.240 8(11)	0.415 2(19)	0.194 0(6)	C(1I)	0.717 3(10)	0.380 8(17)	0.175 7(5)
C(4)	0.242 5(14)	0.487 7(21)	0.221 4(7)	C(2I)	0.780 6(11)	0.349 3(21)	0.193 6(6)
C(5)	0.297 9(11)	0.559 6(18)	0.224 9(5)	C(3I)	0.845 5(13)	0.384 9(25)	0.183 8(7)
C(6)	0.351 5(11)	0.568 0(19)	0.203 6(6)	C(4I)	0.850 4(14)	0.453 5(23)	0.157 6(7)
C(7)	0.349 0(10)	0.497 8(17)	0.176 4(5)	C(5I)	0.791 1(14)	0.482 3(24)	0.139 0(7)
C(8)	0.404 9(9)	0.356 1(16)	0.102 9(5)	C(6I)	0.724 9(12)	0.450 8(20)	0.148 5(6)
C(9)	0.420 1(9)	0.272 9(17)	0.055 9(5)	C(1J)	0.628 6(10)	0.713 1(16)	0.166 6(5)
C(10)	0.414 5(11)	0.220 7(19)	0.023 9(5)	C(2J)	0.606 2(11)	0.688 8(17)	0.199 0(5)
C(11)	0.475 4(13)	0.175 6(22)	0.012 3(6)	C(3J)	0.654 9(14)	0.683 7(21)	0.226 4(6)
C(12)	0.542 1(12)	0.185 7(21)	0.030 3(6)	C(4J)	0.725 0(13)	0.694 0(21)	0.220 2(6)
C(13)	0.550 4(12)	0.240 9(21)	0.060 4(6)	C(5J)	0.751 4(13)	0.714 6(23)	0.190 6(7)
C(14)	0.486 2(11)	0.281 3(18)	0.072 7(5)	C(6J)	0.701 0(11)	0.726 9(22)	0.161 3(6)
C(1A)	0.200 2(12)	−0.011 5(19)	0.151 3(5)	C(1K)	0.524 7(11)	0.844 2(17)	0.130 2(5)
C(2A)	0.149 3(16)	−0.061(3)	0.168 5(9)	C(2K)	0.507 0(13)	0.899 0(20)	0.157 5(6)
C(3A)	0.168 5(18)	−0.131(3)	0.195 1(9)	C(3K)	0.475 8(15)	1.000 8(24)	0.156 7(7)
C(4A)	0.237 3(17)	−0.158(3)	0.201 1(8)	C(4K)	0.458 4(15)	1.040 0(23)	0.125 6(8)
C(5A)	0.287 6(16)	−0.117(3)	0.183 7(8)	C(5K)	0.468 6(16)	0.988 2(25)	0.096 9(7)
C(6A)	0.269 4(15)	−0.042(3)	0.159 5(8)	C(6K)	0.502 5(13)	0.889 7(20)	0.097 6(7)
C(1B)	0.089 4(10)	0.111 7(17)	0.117 5(5)	C(1L)	0.608 8(11)	0.686 5(18)	0.094 2(5)
C(2B)	0.045 0(10)	0.096 0(19)	0.089 7(5)	C(2L)	0.606 4(11)	0.587 6(18)	0.080 2(5)
C(3B)	−0.028 3(14)	0.123 6(25)	0.090 9(8)	C(3L)	0.649 0(15)	0.562 4(22)	0.053 0(7)
C(4B)	−0.052 3(14)	0.176 8(23)	0.117 7(7)	C(4L)	0.690 1(14)	0.646 7(25)	0.041 0(7)
C(5B)	−0.005 3(14)	0.198 7(23)	0.145 7(7)	C(5L)	0.694 4(13)	0.745 0(21)	0.055 0(7)
C(6B)	0.066 7(11)	0.173 6(17)	0.145 1(6)	C(6L)	0.651 3(11)	0.770 2(21)	0.081 1(6)
C(1C)	0.202 1(13)	0.007 8(20)	0.080 3(6)	C(11)	0.050 6(3)	0.317 0(6)	0.236 09(15)
C(2C)	0.168 6(13)	−0.087 7(22)	0.073 1(6)	C(12)	0.745 5(4)	0.065 1(7)	0.077 12(20)
C(3C)	0.184 8(15)	−0.138 8(23)	0.043 0(7)	C(13)	0.483 5(12)	0.182 1(19)	0.291 1(5)
C(4C)	0.231 3(17)	−0.098 3(23)	0.021 7(7)	C(14)	0.390 2(12)	0.204 0(17)	0.224 1(7)
C(5C)	0.265 6(19)	−0.004(3)	0.027 6(8)	C(15)	0.642 4(6)	0.246 4(12)	0.401 5(4)
C(6C)	0.254 0(13)	0.047 7(19)	0.057 9(6)	C(16)	0.538 3(11)	0.358 4(16)	0.363 2(5)
C(1D)	0.104 3(10)	0.471 4(16)	0.068 3(5)	O(1)	0.106 1(15)	0.248(3)	0.227 0(8)
C(2D)	0.105 2(14)	0.430 6(22)	0.100 4(6)	O(2)	0.045 2(15)	0.388 5(22)	0.209 9(6)
C(3D)	0.066 9(14)	0.483 9(23)	0.125 6(6)	O(3)	−0.011 7(14)	0.267(3)	0.237 0(7)
C(4D)	0.035 4(15)	0.577 7(25)	0.117 5(7)	O(4)	0.067 2(16)	0.371(3)	0.264 1(7)
C(5D)	0.033 8(14)	0.623 0(21)	0.084 7(7)	O(5)	0.809 7(11)	0.062(3)	0.061 6(6)
C(6D)	0.072 5(12)	0.566 7(20)	0.060 6(6)	O(6)	0.745 0(15)	0.004 2(22)	0.105 5(6)
C(1E)	0.099 7(10)	0.295 6(15)	0.020 8(5)	O(7)	0.690 7(12)	0.031(3)	0.054 2(7)
C(2E)	0.027 0(11)	0.294 4(19)	0.021 9(6)	O(8)	0.732 9(18)	0.169 8(23)	0.085 8(10)
C(3E)	−0.012 9(11)	0.217 8(21)	0.006 4(7)	O(9)	0.160 7(10)	0.121 3(16)	0.428 3(4)
C(4E)	0.017 7(15)	0.137 9(23)	−0.009 3(7)	C(15)	0.075 3(18)	0.074 (3)	0.467 9(9)
C(5E)	0.092 6(16)	0.128 9(21)	−0.011 8(7)	C(16)	0.103 7(16)	0.154(3)	0.447 3(8)
C(6E)	0.131 9(10)	0.212 7(18)	0.005 0(6)	C(17)	0.185 4(15)	0.195 7(25)	0.406 6(8)
C(1F)	0.163 9(11)	0.495 9(18)	0.001 4(5)	C(18)	0.250 2(16)	0.157(3)	0.388 3(8)
C(2F)	0.119 9(11)	0.478 8(17)	−0.026 7(5)	C(19)	0.421(3)	0.131(5)	0.256 4(16)
C(3F)	0.128 8(13)	0.547 8(22)	−0.054 2(6)	C(20)	0.611(3)	0.370(4)	0.386 5(15)
C(4F)	0.180 5(12)	0.630 3(19)	−0.051 4(6)				

spin-allowed $^1(\pi_2) \longrightarrow {}^1(\pi,\pi^*)$ intraligand transition. There is also a weaker absorption band centred at ≈400 nm, tentatively assigned to the spin-forbidden $^1(\pi_2) \longrightarrow {}^3(\pi,\pi^*)$ transition. Increasing the solvent polarity from MeCN to MeOH leads to a slight red shift in the absorption maximum from 322 to 325 nm.

Upon excitation at 330 nm the free ligand H_2bbzim emits strongly. Fig. 4 shows the emission spectra of a diluted solution ($< 10^{-5}$ mol dm^{-3}) measured in EtOH–MeOH (4:1 v/v) at room temperature and at 77 K. The well resolved vibronic emission almost mirrors the spin-allowed $^1(\pi_2) \longrightarrow {}^1(\pi,\pi^*)$ transition, suggesting that it comes from the fluorescence of the $^1(\pi,\pi^*)$ state. The vibrational progression in the emission spectrum is ≈1350 cm^{-1}, which corresponds to the stretching of the benzimidazole ring.[8]

The emission spectrum of H_2bbzim is strongly affected by its concentration. At 6.4×10^{-5} mol dm^{-3} in dichloromethane the emission is red-shifted to 400 nm. As the electronic absorption spectrum of H_2bbzim does not show any observable dependence on its concentration, such behaviour is not a ground-state phenomenon. Instead, the occurrence of excimeric emission is

Table 4 Selected bond distances (Å) and angles (°) for [{Au(PPh$_3$)}$_2$(μ-bbzim)] with e.s.d.s in parentheses

Au–P	2.228(3)	C(2)–C(3)	1.38(2)
Au–N(1)	2.053(9)	C(2)–C(7)	1.42(2)
N(1)–C(1)	1.38(1)	C(3)–C(4)	1.36(2)
N(1)–C(2)	1.40(2)	C(4)–C(5)	1.36(2)
N(2)–C(1)	1.32(2)	C(5)–C(6)	1.38(2)
N(2)–C(7)	1.40(2)	C(6)–C(7)	1.38(2)
C(1)–C(1)	1.44(2)		
P–Au–N(1)	176.9(3)	N(1)–C(2)–C(7)	106(1)
Au–N(1)–C(1)	127.1(7)	C(3)–C(2)–C(7)	122(1)
Au–N(1)–C(2)	125.2(7)	C(2)–C(3)–C(4)	118(1)
C(1)–N(1)–C(2)	105.5(9)	C(3)–C(4)–C(5)	121(1)
C(1)–N(2)–C(7)	105.3(9)	C(4)–C(5)–C(6)	122(1)
N(1)–C(1)–N(2)	114.0(9)	C(5)–C(6)–C(7)	119(1)
N(1)–C(1)–C(1)	121(1)	N(2)–C(7)–C(2)	109(1)
N(2)–C(1)–C(1)	125(1)	N(2)–C(7)–C(6)	133(1)
N(1)–C(2)–C(3)	132(1)	C(2)–C(7)–C(6)	118(1)

Table 5 Selected bond distances (Å) and angles (°) for [{Au(PPh$_3$)}$_4$(μ-bbzim)][ClO$_4$]$_2$ with e.s.d.s in parentheses

Au(1)–Au(2)	3.157(1)	N(4)–C(8)	1.33(2)
Au(1)–P(1)	2.236(6)	N(4)–C(14)	1.41(3)
Au(1)–N(1)	2.03(2)	C(1)–C(8)	1.44(3)
Au(2)–P(2)	2.233(5)	C(2)–C(3)	1.38(3)
Au(2)–N(2)	2.05(1)	C(2)–C(7)	1.42(3)
Au(3)–Au(4)	3.222(1)	C(3)–C(4)	1.41(4)
Au(3)–P(3)	2.239(5)	C(4)–C(5)	1.37(4)
Au(3)–N(4)	2.06(1)	C(5)–C(6)	1.34(3)
Au(4)–P(4)	2.233(5)	C(6)–C(7)	1.39(3)
Au(4)–N(3)	2.06(2)	C(9)–C(10)	1.43(3)
N(1)–C(1)	1.34(3)	C(9)–C(14)	1.38(3)
N(1)–C(2)	1.37(2)	C(10)–C(11)	1.37(3)
N(2)–C(8)	1.33(2)	C(11)–C(12)	1.41(3)
N(2)–C(9)	1.39(3)	C(12)–C(13)	1.38(3)
N(3)–C(1)	1.36(3)	C(13)–C(14)	1.41(3)
N(3)–C(7)	1.41(2)		
Au(2)–Au(1)–P(1)	108.8(1)	N(1)–C(1)–C(8)	124(2)
Au(2)–Au(1)–N(1)	78.2(5)	N(3)–C(1)–C(8)	123(2)
P(1)–Au(1)–N(1)	172.3(5)	N(1)–C(2)–C(3)	133(2)
Au(1)–Au(2)–P(2)	110.3(1)	N(1)–C(2)–C(7)	109(2)
Au(1)–Au(2)–N(2)	75.5(4)	C(3)–C(2)–C(7)	118(2)
P(2)–Au(2)–N(2)	173.9(5)	C(2)–C(3)–C(4)	119(2)
Au(4)–Au(3)–P(3)	110.3(2)	C(3)–C(4)–C(5)	119(2)
Au(4)–Au(3)–N(4)	78.4(4)	C(4)–C(5)–C(6)	125(2)
P(3)–Au(3)–N(4)	171.2(4)	C(5)–C(6)–C(7)	116(2)
Au(3)–Au(4)–P(4)	111.6(2)	N(3)–C(7)–C(2)	106(2)
Au(3)–Au(4)–N(3)	73.3(4)	N(3)–C(7)–C(6)	131(2)
P(4)–Au(4)–N(3)	174.7(5)	C(2)–C(7)–C(6)	123(2)
Au(1)–N(1)–C(1)	129(1)	N(2)–C(8)–N(4)	114(2)
Au(1)–N(1)–C(2)	124(1)	N(2)–C(8)–C(1)	122(2)
C(1)–N(1)–C(2)	107(2)	N(4)–C(8)–C(1)	124(2)
Au(2)–N(2)–C(8)	129(1)	N(2)–C(9)–C(10)	132(2)
Au(2)–N(2)–C(9)	125(1)	N(2)–C(9)–C(14)	109(2)
C(8)–N(2)–C(9)	105(1)	C(10)–C(9)–C(14)	120(2)
Au(4)–N(3)–C(1)	130(1)	C(9)–C(10)–C(11)	117(2)
Au(4)–N(3)–C(7)	123(1)	C(10)–C(11)–C(12)	122(2)
C(1)–N(3)–C(7)	106(2)	C(11)–C(12)–C(13)	123(2)
Au(3)–N(4)–C(8)	127(1)	C(12)–C(13)–C(14)	114(2)
Au(3)–N(4)–C(14)	125(2)	N(4)–C(14)–C(9)	106(2)
C(8)–N(4)–C(14)	106(2)	N(4)–C(14)–C(13)	129(2)
N(1)–C(1)–N(3)	113(2)	C(9)–C(14)–C(13)	124(2)

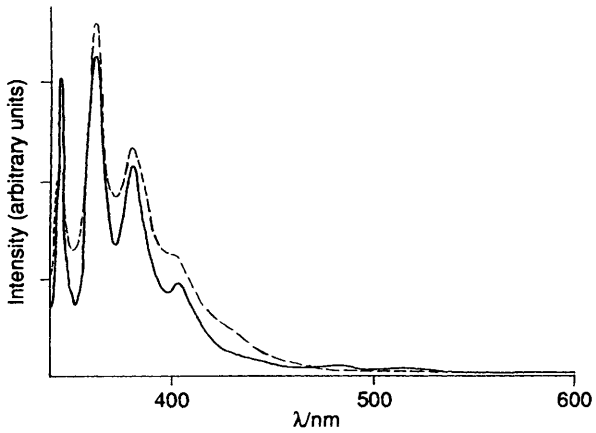

Fig. 4 Emission spectra of H_2bbzim in EtOH–MeOH (4:1 v/v) fluid solution (– – – –) at room temperature and glass (——) at 77 K

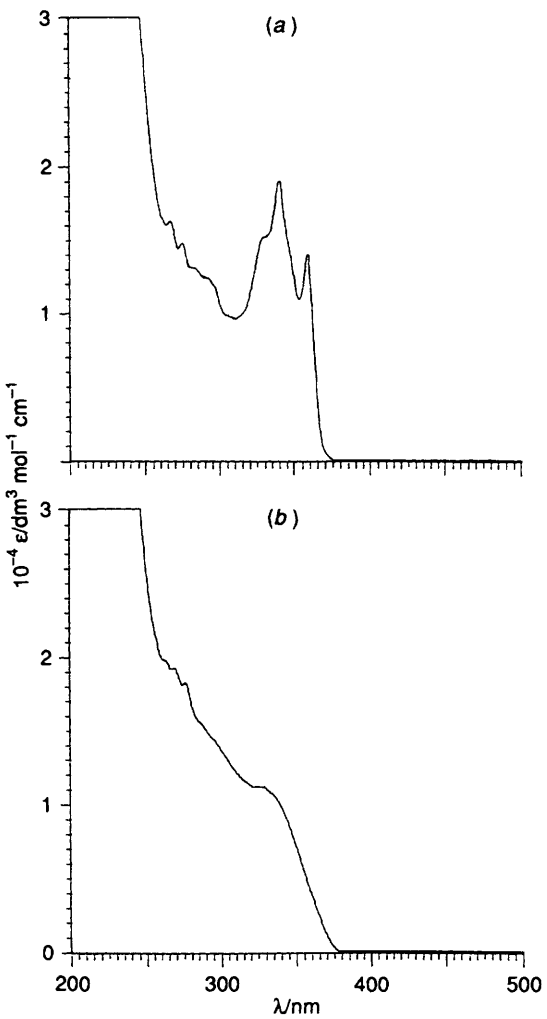

Fig. 5 The UV/VIS absorption spectra of (*a*) [{Au(PPh$_3$)}$_2$(μ-bbzim)] and (*b*) [{Au(PPh$_3$)}$_4$(μ-bbzim)][ClO$_4$]$_2$ in CH_2Cl_2 at room temperature

suggested. In accordance with this, the emission lifetime monitored at 360 nm and concentration of H_2bbzim were found to obey the Stern–Volmer equation $1/t = (1/t_0) + k_q[H_2\text{bbzim}]$, with the self quenching rate constant (k_q) determined to be 6.0×10^9 dm^3 mol^{-1} s^{-1} in dichloromethane at room temperature. Even at high dilution, the emission lifetime of H_2bbzim is tens of microseconds which is significantly longer than that in the general case of prompt fluorescence.[9] We suggest that this is due to thermally induced delayed fluorescence.[10,11]

Spectroscopic and Photophysical Properties of the Complexes.—The spectroscopic and photophysical properties of the gold(I) complexes together with H_2 bbzim are listed in Table 6. Fig. 5(*a*) and 5(*b*) show the UV/VIS absorption spectra

Table 6 Photophysical data in dichloromethane at room temperature

	H_2bbzim	$[\{Au(PPh_3)\}_2(\mu\text{-bbzim})]$	$[\{Au(PPh_3)\}_4(\mu\text{-bbzim})][ClO_4]_2$
λ_{max}^{abs}/nm	313 (32.0)	340 (1.94)	325 (1.12)
(10^{-4} ε_{max}/dm^3 mol^{-1} cm^{-1})	322 (46.1)	359 (1.40)	
	339 (42.9)		
	386 (6.38)		
	409 (7.99)		
	434 (4.78)		
λ_{max}^{em}/nm	346	366	346
	364	382	366
	381	401	382
		444	464(sh)
		473	491
		504	
τ/μs	13	15	62

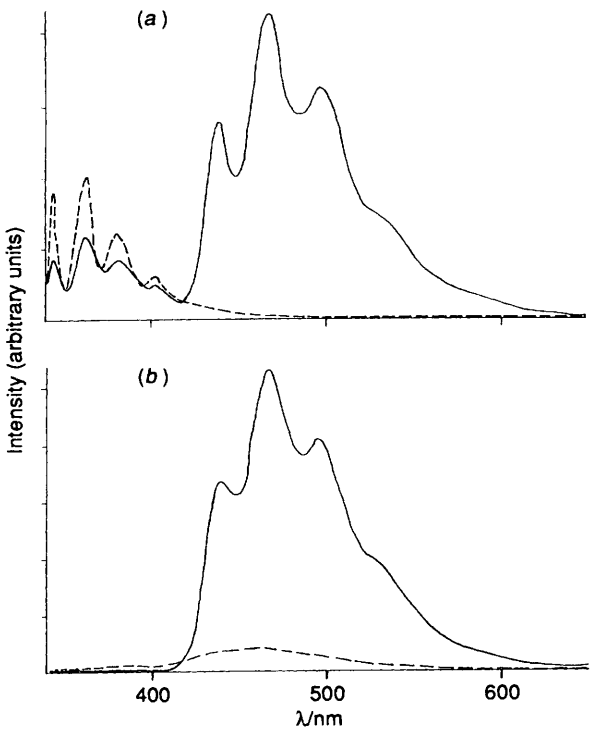

Fig. 6 Emission spectra of (*a*) $[\{Au(PPh_3)\}_2(\mu\text{-bbzim})]$ and (*b*) $[\{Au(PPh_3)\}_4(\mu\text{-bbzim})][ClO_4]_2$ in EtOH–MeOH (4:1 v/v) fluid solution (- - - -) at room temperature and glass (——) at 77 K

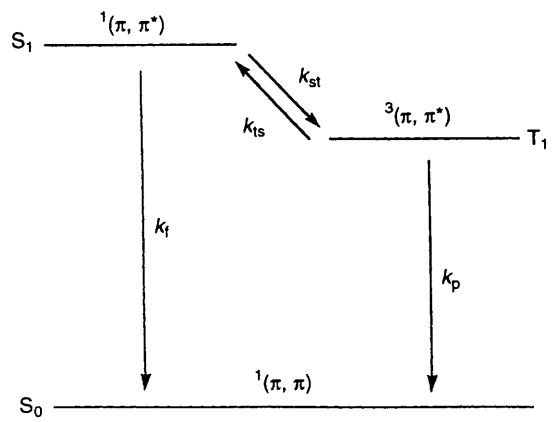

Scheme 1

of $[\{Au(PPh_3)\}_2(\mu\text{-bbzim})]$ **1** and $[\{Au(PPh_3)\}_4(\mu\text{-bbzim})][ClO_4]_2$ **2**. Both spectra display intense absorptions at 300–370 nm, which are less resolved for **2** than **1**. These absorption bands are assigned to the intraligand $^1(\pi_2) \longrightarrow {}^1(\pi,\pi^*)$ transition, perturbed through co-ordination to gold(I).

Complexes **1** and **2** show intense emission upon excitation at 330 nm as shown in Figs. 6(*a*) and 6(*b*). Besides the fluorescence at 340–430 nm, a lower-energy emission is also found in each case. The latter bands are attributable to phosphorescence from the $^3(\pi,\pi^*)$ state. The difference in energy between the $^1(\pi,\pi^*)$ and $^3(\pi,\pi^*)$ states is about 5900 cm^{-1} for **1** and **2**. These values are small and hence may account for the observed thermally induced delayed fluorescence, which is favoured in molecules having a small singlet–triplet energy gap.

When a solution of complex **1** or **2** in EtOH–MeOH (4:1 v/v) is cooled to 77 K the fluorescence decreases in intensity for **1** or disappears for **2** as illustrated in Figs 6(*a*) and 6(*b*). These findings are explained in Scheme 1.

The co-ordination of gold(I) to bbzim^{2-} may facilitate all spin-forbidden transitions (intersystem crossings and phosphorescence) but does not affect spin-allowed transitions (such as fluorescence).[9] Therefore the rate constants k_{st}, k_{ts} and k_p should be increased by the heavy-atom effect but not k_f. Thus it is not unreasonable to find both fluorescence and phosphorescence in the metal complexes but only fluorescence in the free ligand. At low temperature, k_{ts} is too slow to compete with k_p and hence the intensity of phosphorescence is enhanced (as shown in Fig. 6). The phosphorescence lifetimes of complexes **1** and **2** at room temperature in dichloromethane were also found to depend on the complex concentration according to the Stern–Volmer equation. The self-quenching rate constants are 1.5×10^8 and 1.8×10^8 dm^3 mol^{-1} s^{-1} for **1** and **2**, respectively. The phosphorescence lifetimes of **1** and **2** at infinite dilution were estimated from the Stern–Volmer plots to be 15 and 62 μs, respectively.

Acknowledgements

We acknowledge support from the National Science Council of Taiwan and the Hong Kong Research Grants Council. C. M. C. and D. L. are grateful for a visiting professorship and a scholarship, administered by the National Taiwan University and Li Ka Shing Scholarship Foundation, respectively.

References

1 T. M. McCleskey and H. B. Gray, *Inorg. Chem.*, 1992, **31**, 1733.
2 C. M. Che, H. L. Kwong, V. W. W. Yam and K. C. Cho, *J. Chem. Soc., Chem. Commun.*, 1989, 885; C. M. Che, H. L. Kwong, C. K. Poon and V. W. W. Yam, *J. Chem. Soc., Dalton Trans.*, 1990, 3741; V. W. W. Yam, T. F. Lai and C. M. Che, *J. Chem. Soc., Dalton Trans.*, 1990, 3747; C. M. Che., H. K. Yip, V. W. W. Yam, P. Y. Cheung, T. F. Lai, S. T. Shieh, and S. M. Peng, *J. Chem. Soc., Dalton Trans.*, 1992, 427; D. Li, C. M. Che, S. M. Peng, S. T. Liu, Z. Y. Zhou and T. C. W. Mak, *J. Chem. Soc., Dalton Trans*, 1993, 189.

3 C. King, J. C. Wang, Md. N. I. Khan and J. P. Fackler, jun., *Inorg. Chem.*, 1989, **28**, 2145; Md. N. I. Khan, C. King, D. Heinrich, J. P. Fackler, jun. and L. C. Porter, *Inorg. Chem.*, 1989, 28, 2150.
4 B. F. Fieselmann, D. N. Hendrickson and G. D. Stucky, *Inorg. Chem.*, 1978, **17**, 2078.
5 R. Uson, J. Gimeno, J. Fornies, F. Martinez and C. Fernandez, *Inorg. Chim. Acta*, 1981, **54**, L95; 1982, **63**, 91.
6 E. J. Gabe, Y. LePage, J. P. Charland, F. L. Lee and P. S. White, *J. Appl. Crystallogr.*, 1989, **22**, 384.
7 R. Uson, L. A. Oro, J. Gimeno, M. A. Ciriano, J. A. Cabeza, A. Tiripicchio and M. T. Camellini, *J. Chem. Soc., Dalton Trans.*, 1983, 323; M. P. Garcia, A. M. Lopez, M. A. Esteruelas, F. J. Lahoz and L. A. Oro, *J. Chem. Soc., Dalton Trans.*, 1990, 3465.
8 R. Uson, J. Gimeno, J. Fornies and F. Martinez, *Inorg. Chim. Acta*, 1981, **50**, 173.
9 N. J. Turro, in *Modern Molecular Photochemistry*, University Science Books, Mill Valley, CA, 1991.
10 J. Saltiel, H. C. Curtis, L. Metts, J. W. Miley, J. Winterle and M. Wrighton, *J. Am. Chem. Soc.*, 1970, **92**, 410.
11 R. E. Brown, L. A. Singer and J. H. Parks, *Chem. Phys. Lett.*, 1972, **14**, 193.

Received 12*th January* 1993; *Paper* 3/00194F